

Quantum Pinch Effect

Manvir S. Kushwaha

Department of Physics and Astronomy, Rice University, P.O. Box 1892, Houston, TX 77251, USA

(Dated: October 3, 2018)

We investigate a two-component, cylindrical, quasi-one-dimensional quantum plasma subjected to a *radial* confining harmonic potential and an applied magnetic field in the symmetric gauge. It is demonstrated that such a system as can be realized in semiconducting quantum wires offers an excellent medium for observing the quantum pinch effect at low temperatures. An exact analytical solution of the problem allows us to make significant observations: surprisingly, in contrast to the classical pinch effect, the particle density as well as the current density display a *determinable* maximum before attaining a minimum at the surface of the quantum wire. The effect will persist as long as the equilibrium pair density is sustained. Therefore, the technological promise that emerges is the route to the precise electronic devices that will control the particle beams at the nanoscale.

PACS numbers: 73.63.Nm, 52.55.Ez, 52.58.Lq, 85.35.Be

The pinch effect is one of the most fascinating phenomena in plasma physics with immense applications to the problems of peace and war. It is the manifestation of radial constriction of a compressible conducting plasma [or a beam of charged particles] due to the magnetic field generated by the parallel electric currents. Cylindrical symmetry is central to the realization of the effect. In the literature, the phenomenon is also referred to as self-focusing, magnetic pinch, plasma pinch, or Bennett pinch. The pinch effect in the cylindrical geometry is classified after the direction in which the current flows: In a θ -pinch, the current is azimuthal and the magnetic field axial; in a z -pinch, the current is axial and the magnetic field azimuthal; in a screw (or θ - z) pinch, an effort is made to combine both θ -pinch and z -pinch [see Fig. 1].

While a popular reference dates back to 1790 when Martinus van Marum in Holland created an explosion by discharging 100 Leyden jars into a wire, the first formal study of the effect was not undertaken until 1905 when Pollock and Barraclough [1] investigated a compressed and distorted copper tube after it had been struck by lightning. They argued that the magnetic forces due to the large current flow could have caused the compression and distortion. Shortly thereafter, Northrup published a similar but independent diagnosis of the phenomenon in liquid metals [2]. However, the major breakthrough in the topic came with the publication of the derivation of the radial pressure balance in a static z -pinch by Bennett [3]. Curiously enough, the term “pinch effect” was only coined in 1937 by Tonks in his work on the high current densities in low pressure arcs [4]. This was followed by a *first* patent for a fusion reactor based on a toroidal z -pinch submitted by Thompson and Blackman [5]. The subsequent progress – theoretical and experimental – on the pinch effect in the gas discharges was driven by the quest for the controlled nuclear fusion.

Needless to say, the plasma commands a glamorous status in the physics literature by representing the

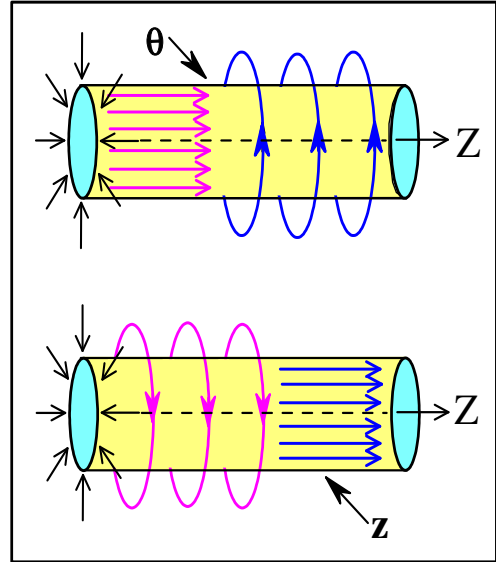


FIG. 1: (Color online) The schematics of the θ -pinch (the upper panel) and the z -pinch (the lower panel). The curves in blue (magenta) refer to the current (magnetic field).

fourth state of matter. Our key interest here is in the solid state plasmas (SSP), which share several characteristic features with but are also known to have quantitative differences from the gaseous space plasmas (GSP). The GSP is ill-famed for two inherently juxtaposing characteristics: confinement and instability. The SSP is, on the contrary, a uniform, equilibrium system tightly bound to the lattice where the boundary conditions make no sense, whereas in GSP they can be crucial. Notice that only two-component, semiconductor SSP with approximately equal number of electrons and holes can support a significant pinching. For a single mobile carrier the space-charge electric field due to any alteration in the charge-density will impede such inward motion. Thus a metal with only

electrons contributing to the conduction is a poor option. The 1960's had seen considerable experimental [6-15] and theoretical [16-19] efforts focused on studying pinch effect in the bulk SSP, with instabilities manifesting themselves as voltage and current oscillations at frequencies up to 50 MHz.

Notwithstanding the SSP had been imbued to a greater extent by the research pursuit for the pinch effect in the GSP, the subject did not gain sufficient momentum because the early 1970's had begun to offer the condensed matter physicists with the new venues to explore: the semiconducting quantum structures with reduced dimensions such as quantum wells, quantum wires, quantum dots, and their periodic counterparts. The continued tremendous research interest in these quasi-n-dimensional electron gas [Q-nDEG] systems can now safely be accredited to the discovery of the quantum Hall effects – both integral [20] and fractional [21]. The fundamental issue behind the excitement in these man-made nanostructures lies in the fact that the charge carriers exposed to external probes such as electric and/or magnetic fields can exhibit unprecedented quantal effects that strongly modify their behavior characteristics [22]. To what extent these effects can influence the behavior of a quantum wire [or, more realistically, Q-1DEG system] in the cylindrical symmetry, which offers a quantum analogue of the classical structure subjected to investigate the pinch effect in the conventional SSP [or GSP], has not, to our knowledge, been explored. This is the motivation behind the present work.

We consider a two-component, quasi-1DEG system characterized by a radial harmonic confining potential and subjected to an applied (azimuthal and axial) magnetic field in the cylindrical symmetry. The two-component Q-1DEG systems are comprised of both types of charge carriers [i.e., electrons and holes] and are known to have been fabricated in a wide variety of semiconducting quantum wires by optical pumping techniques [23-25]. In the linear response theory, the resultant system is characterized by the single-particle Hamiltonian $H = H_0 + H_1$, where [after Peierls substitution $\mathbf{p} \rightarrow (\mathbf{p} \pm \frac{e}{c}\mathbf{A})$, with $\mathbf{A} = \mathbf{A}_0 + \mathbf{A}_1$]

$$H_0 = \frac{1}{2}m_e\mathbf{v}_e^2 + \frac{1}{2}m_h\mathbf{v}_h^2 + \frac{1}{2}m_e\omega_e^2r^2 + \frac{1}{2}m_h\omega_h^2r^2, \quad (1)$$

$$H_1 = \frac{e}{2c}[(\mathbf{v}_e \cdot \mathbf{A}_1 + \mathbf{A}_1 \cdot \mathbf{v}_e) - (\mathbf{v}_h \cdot \mathbf{A}_1 + \mathbf{A}_1 \cdot \mathbf{v}_h)], \quad (2)$$

to first order in \mathbf{A}_1 . Here c is the speed of light in vacuum and $-e(+e)$, $m_e(m_h)$, and $\omega_e(\omega_h)$ are, respectively, the electron (hole) charge, mass, and the characteristic frequency of the harmonic oscillator. $\mathbf{v}_i = \frac{1}{m_i}(\mathbf{p} \pm \frac{e}{c}\mathbf{A}_0)$ is the velocity operator for an electron (hole). A few significant aspects of the formalism are: (i) the formal Peierls substitution, by which a magnetic field is introduced into the Hamiltonian, is a direct consequence of gauge invariance under the transformation $\psi \rightarrow \psi e^{i\phi}$, with ϕ being an arbitrary phase, (ii) in the Coulomb gauge $\nabla \cdot \mathbf{A} = 0 \Rightarrow \mathbf{A} \cdot \mathbf{p} = \mathbf{p} \cdot \mathbf{A}$, and (iii)

we choose symmetric gauge, which is quite popular in the many-body theory, defined by $\mathbf{A}_0 = B(0, \frac{1}{2}r, 0)$.

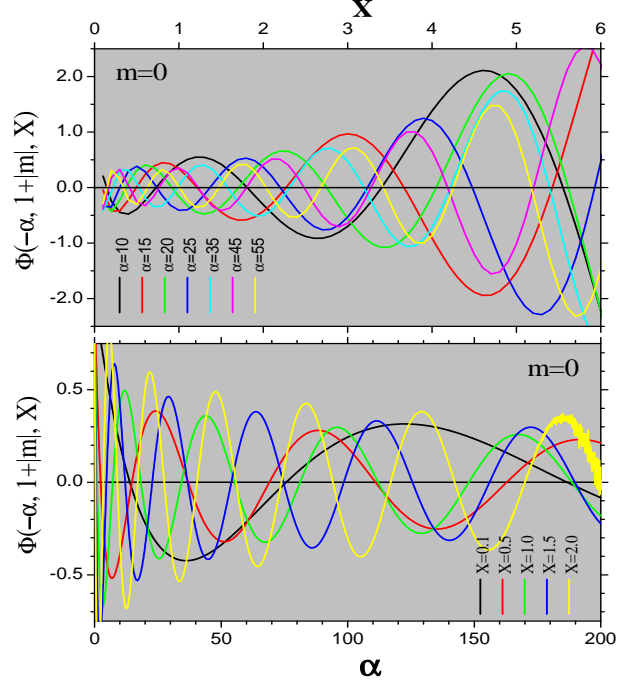


FIG. 2: (Color online) The plot of the CHF $\Phi(\alpha, 1+|m|, X)$ vs. X (the upper panel) and α (the lower panel), for $m = 0$.

Next, we consider, for the sake of simplicity, the quantization energy for the electrons equal to that for the holes implying that $\omega_e = \omega_o = \omega_h$. Then, in the cylindrical coordinates $[(r, \theta, z)]$, the Schrödinger equation $H_0\psi = \epsilon\psi$ for a quantum wire of radius R and length L is solved to characterize the system with the eigenfunction $\psi(r, \theta, z) = \psi(r)\psi(\theta)\psi(z)$, where

$$\psi(z) = \sqrt{\frac{2}{L}} \sin(kz), \quad \text{with } k = n\pi/L, \quad (3)$$

$$\psi(\theta) = \sqrt{\frac{1}{2\pi}} e^{im\theta}, \quad (4)$$

$$\psi(r) = \frac{N}{s^{|m|/2}} e^{-X/2} X^{|m|/2} \Phi(-\alpha; 1+|m|; X), \quad (5)$$

where n is an integer, $m = 0, \pm 1, \pm 2, \dots$ is the azimuthal quantum number, $s = \sqrt{m_+/ \mu}$, and $X = r^2/(2\ell_c^2)$, with $\ell_c = \sqrt{\hbar/\mu\Omega_+}$ as the effective magnetic length in the problem, $m_+ = m_e + m_h$ as the total mass, $\mu = m_em_h/(m_e + m_h)$ as the reduced mass, $\Omega_+ = s\Omega = s\sqrt{\omega_{ce}\omega_{ch} + 4\omega_o^2}$ as the effective hybrid frequency, and $\omega_{ci} = eB/(m_i c)$ as the cyclotron frequency. In Eq. (5), N is the normalization coefficient to be determined by the condition $\int_0^R dr r |\psi(\dots)|^2 = 1$, which yields

$$N^{-2} = \frac{\ell_c^2}{s^{|m|}} \int_0^\zeta dX e^{-X} X^{|m|} [\Phi(-\alpha; 1+|m|; X)]^2 \quad (6)$$

where the upper limit $\zeta = R^2/2\ell_c^2$. In Eq. (5), $\Phi(-\alpha; 1+|m|; X)$ is the confluent hypergeometric func-

tion (CHF) [26], which is a solution of the Kummer's equation: $XU'' + [1 + |m| - X]U' + \alpha U = 0$, where $\alpha = \frac{1}{\hbar\Omega_+}[\epsilon - \frac{\hbar^2 k^2}{2\mu} - \frac{m}{2}\hbar\Omega_-] - \frac{1}{2}(1 + |m|)$, with $\Omega_- = (\omega_{ce} - \omega_{ch})$ being the effective cyclotron frequency. The wavefunction $\psi(\dots)$ obeys the boundary condition $\psi(r = R) = 0 \Rightarrow \Phi(-\alpha; 1 + |m|; \zeta) = 0$, which yields

$$\frac{\epsilon'}{\epsilon_r} = \zeta \left[\alpha + \frac{1}{2} (1 + m \frac{\Omega_-}{\Omega_+} + |m|) \right] \quad (7)$$

where $\epsilon' = \epsilon - \frac{\hbar^2 k^2}{2\mu}$ and $\epsilon_r = 2\hbar^2/(\mu R^2)$. It is needless to state that the term $\frac{\hbar^2 k^2}{2\mu}$ is only additive and hence inconsequential. What is important to notice though is that, for a given m , ζ and α are determined self-consistently where $\Phi(-\alpha; 1 + |m|; X) = 0$. Figure 2 demonstrates that $\Phi(\dots)$ is unambiguously a well-behaved function over a wide range of X and α and that its period is seen to be decreasing with increasing X or α as the case may be. Since the rest of the illustrative examples require the quantum wire to be specified, we choose GaAs/Ga_{1-x}Al_xAs system: $m_e = 0.067m_0$, $m_h = 0.47m_0$, and the aspect ratio $r_a = L/R = 10^3$ [27]. Another important parameter in the problem is the reduced magnetic flux ϕ/ϕ_0 : the ratio of the magnetic flux $[\phi = B\pi R^2]$ to the quantum flux $[\phi_0 = hc/e] -$ yielding $\phi/\phi_0 = \zeta$.

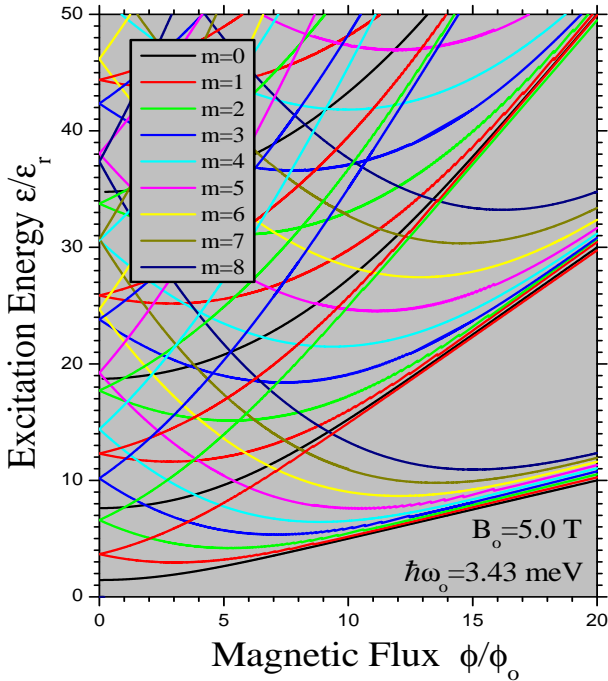


FIG. 3: (Color online) The excitation spectrum for a (finite) cylindrical quantum wire subjected to a magnetic field in the symmetric gauge. The y (x) axis refers to the reduced energy (reduced magnetic flux). The lower (upper) arm of a wedge corresponds to a negative (positive) value of m .

Figure 3 illustrates the excitation spectrum for the cylindrical quantum wire of finite length as a function

of the reduced magnetic flux ϕ/ϕ_0 , for several values of m . This is a result of (involved) computation based on Eq. (7) within the strategy as stated above. The parameters used are as listed inside the picture. For every m , the lower (upper) branch of the wedge corresponds to the negative (positive) value of m . It is interesting to see that both arms of each wedge gradually approach the Landau levels at higher magnetic flux, just as in the case of the Fock-Darwin spectrum of a quantum dot [see, e.g., Ref. 22]. Notice that this is not a mere coincidence, rather a consequence of the isomorphism in the expression of the single-particle energies for the two quantum systems.

Next, we proceed to solve the time-dependent Schrodinger equation in order to derive the equation of continuity: $\frac{\partial \rho}{\partial t} + \nabla \cdot \mathbf{J} = 0$, where the electrical current density \mathbf{J} is given by [with $m_e < m_h$]

$$\mathbf{J} = \frac{ie\hbar}{2m_e} (\psi \nabla \psi^* - \psi^* \nabla \psi) + \frac{e^2}{m_e c} \mathbf{A} \psi^* \psi, \quad (8)$$

where the vector potential $\mathbf{A} [= \mathbf{A}_0 + \mathbf{A}_1]$ is approximated such that we seek to measure its *ac* part (\mathbf{A}_1) just as we do its *dc* one (\mathbf{A}_0), i.e., we express \mathbf{A}_0 in the symmetric gauge just as before and $\mathbf{A}_1 = B(0, 0, r)$. This is not to say that there aren't other, more subtle, ways to complicate the situation, but since this is the first paper of its kind, we choose to stick to the bare-bone simplicity – the complexity will (and should) come later. Consequently, it is not difficult to split Eq. (8) into its scalar components. The result is

$$\begin{aligned} J_\theta &= \left[\frac{e\hbar m}{m_e r} + \frac{e^2 B r}{2s m_e} \right] |\psi(r, \theta, z)|^2 \\ J_z &= \frac{e^2 B r}{s m_e} |\psi(r, \theta, z)|^2. \end{aligned} \quad (9)$$

The very nature of the magnetic field – with its charismatic role in localizing the charge carriers in the plane perpendicular to its orientation – elucidates why the radial component of the current density $J_r = 0$. It is interesting to notice that in the absence of the z component of \mathbf{A}_1 , J_z will be zero for a quantum wire of *finite* length (as is the case here). This is contrary to the case of a wire of an *infinite* length – where $J_z \neq 0$ even when $[\mathbf{A}_1]_z = 0$. Equations (9) should, in principle, provide the clue to the quest in the problem.

Figure 4 shows the 1D particle density (n_{1D}) in the quantum wire as a function of the reduced radius for various values of the magnetic field (left panel) and confinement potential (right panel). The confinement potential in the left panel is $\hbar\omega_0 = 1.0$ meV and the magnetic field in the right panel is $B = 1.0$ T. The Other parameters are listed inside the picture. The particle density shows a maximum. We were able to find out that this maximum occurs unequivocally at $\frac{d}{dr}[n_{1D}] = \frac{d}{dr}[r\Phi^2(\alpha, 1 + |m|, X)] = 0 \Rightarrow r/R = 1/\sqrt{2\zeta} = 0.3271$. Since the particle density is fundamental to most of the electronic, optical, and transport properties, we expect the current features to make a

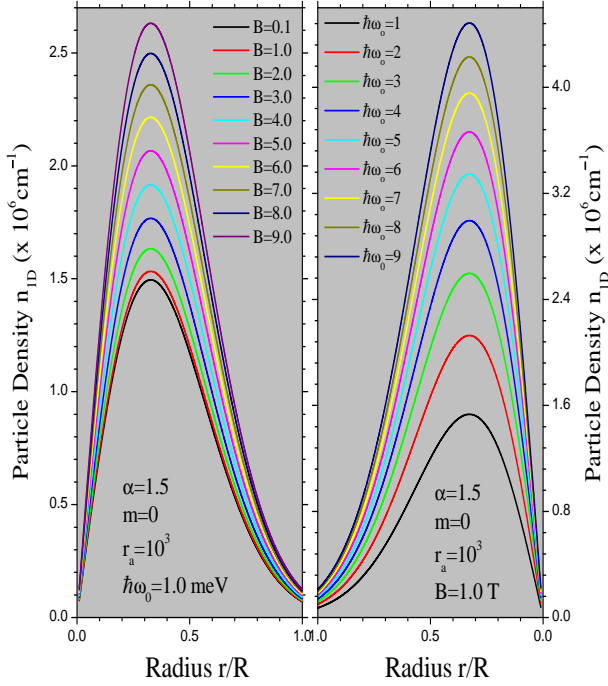


FIG. 4: (Color online) The particle density n_{1D} as a function of the reduced radius r/R for the several values of the magnetic field (left panel) and confinement potential (right panel). The parameters are as listed inside the picture. Again, it is a GaAs/Ga_{1-x}Al_xAs quantum wire.

mark in those phenomena, at least, in the cylindrical symmetry. In a quantum system the particle density has much to do with the Fermi energy in the system. For the fact that each quantum level can take two electrons with opposite spin, the Fermi energy ϵ_F of a system of \mathcal{N} noninteracting electrons for a *finite* system at absolute zero temperature is equal to the energy of the $\frac{1}{2}\mathcal{N}$ -th level. As such, one can compute self-consistently the Fermi energy in a *finite* quantum wire containing \mathcal{N} electrons through this expression: $\mathcal{N} = 2 \sum_m \theta(\epsilon_F - \epsilon'_m)$, where $\theta(\dots)$ is the Heaviside step function and the summation is only over the azimuthal quantum number m . The prime on ϵ_m has the same meaning as explained before. Because the electronic excitation spectrum happens to be so very intricate [see Fig. 3], the Fermi energy will not be a smooth function of the magnetic field (or flux). This intricacy should also lead to complex structures in the magnetotransport phenomena.

Figure 5 depicts the current density as a function of the reduced radius for several values of the magnetic field. The parameters used are: the confinement potential $\hbar\omega_0 = 1.0$ meV, aspect ratio $r_a = 1000$, $\alpha = 1.5$, and $kz = 1.8^\circ$. Other material parameters are the same as before. We observe that the larger the magnetic field, the greater the current density. This is what we should expect intuitively: the larger the magnetic field, the stronger the confinement of the charge carriers near the axis and hence greater the

current density. The most important aspect this figure reveals is that there is a maximum in the current density and this maximum is again defined exactly by $r/R = 0.3271$. In a certain way, Fig. 4 substantiates the features observed in Fig. 5. This tells us that in a quantum wire the maximum of charge density lies at $r/R = 0.3271$ instead of exactly at the axis. Note that the classical pinch effect in conventional (3D) SSP [6-19] does not share any such feature. Very close to the axis and to the surface of the quantum wire, the minimum of the current density is smallest but still nonzero. Traditionally, θ -pinches ($\Rightarrow J_\theta$) tend to resist the plasma instabilities due to the famous *frozen-in-flux* theorem [28], whereas z -pinches ($\Rightarrow J_z$) tend to favor the confinement phenomena. The magnitude of J_z is double of that of the J_θ just as dictated by Eqs. (9). We believe that these currents are of moderate strength and would not cause an undue heating of the two-component plasma in the quantum wires which are generally subjected to experimental observations at low temperatures.

There are several other important (and interrelated) issues such as the equilibrium, temperature, recombination, and population inversion, which would certainly give a better insight into the problem. The aspect of population inversion enabling the magnetized quantum wires to act as optical amplifiers has recently been discussed in a different context [29]. These issues are deferred to a future publication.

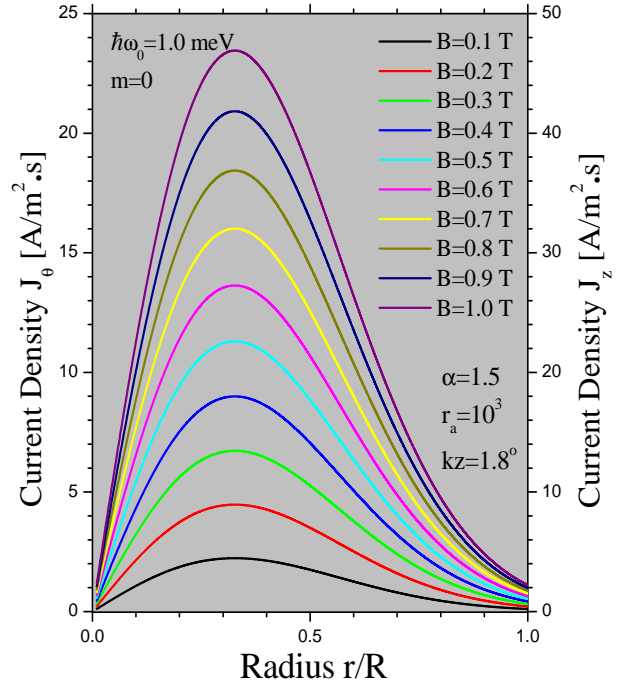


FIG. 5: (Color online) The current density J_θ (J_z) on the left (right) vertical axis vs. the reduced radius r/R for the several values of the magnetic field. The parameters used are: $\hbar\omega_0 = 1.0$ meV, aspect ratio $r_a = 1000$, $\alpha = 1.5$, and $kz = 1.8^\circ$. We consider a GaAs/Ga_{1-x}Al_xAs quantum wire just as before.

In summary, we have investigated the quantum analogue of the classical pinch effect in finite quantum wires with cylindrical symmetry. Since the late 1940s the pinch effect in a gas discharge has been investigated intensively in laboratories throughout the world, because it offers the possibility of achieving the magnetic confinement of a hot plasma (a highly ionized gas) necessary for the successful operation of a thermonuclear or fusion reactor. In solid state plasmas the issues related to confinement, as discussed above, are not encountered. However, since no system provides an ideal environment in the real world, the SSPs also pose challenges. In a conventional SSP with no impurities, the thermally excited pair density is a function of temperature only. Any deviation from this (thermal) equilibrium can (and, generally, does) give rise to recombination, which, in turn, affects the pinching process. The desired maintenance of the equilibrium pair density occurs through various processes such as Coulomb interactions and particle-lattice interactions, which are not independent and hence cause unintended consequences. The quantum wires are the systems in which most of the experiments are performed at low (close to zero) temperatures. Therefore, the risks of thermal non-equilibrium and recombination are much smaller than those ordinarily encountered in conventional SSP. This implies that two-component quantum wires at low temperatures offer an ideal platform for the realization of the quantum pinch effect.

Myriad of applications of quantum pinches bud out from the very thought of the self-focused, two-component plasma in a quantum wire with cylindrical symmetry. The plasma by definition is electrically conductive implying that it responds strongly to electromagnetic fields. The self-focusing (or pinching) only adds to the response. The quantum wire brings all this to the nanoscale. Therefore, we are designing an electronic device that can (and will) control the particle beams at the nanoscale. Potential applications include extremely refined nanoswitches, nanoantennas, optical amplifiers, and precise particle-beam nanoweapons, just to name a few. The greatest advantage of the quantum pinch effect over its classical counterpart is that it offers a Gaussian-like cycle of operation with two minima passing through a maximum. The smooth functionality of the plasma devices is, however, based on a single tenet: there must be means not only to produce it, but also to sustain it.

The author feels grateful to L.N. Pfeiffer who affirmed the feasibility of achieving the aspect ratio of $r_a = 1000$ in the semiconducting quantum wires within the current technology and for the fruitful discussions. I would also like to thank H. Sakaki, Naomi Halas, and Peter Nordlander for stimulating discussions on various aspects related to the subject. He is appreciative of Kevin Singh for the invaluable help with the software during this investigation.

-
- [1] J.A. Pollock and S. Barraclough, Proc. Roy. Soc. (New South Wales) **39**, 131 (1905).
 - [2] E.F. Northrup, Phys. Rev. **24**, 474 (1907).
 - [3] W.H. Bennett, Phys. Rev. **45**, 890 (1934).
 - [4] L. Tonks, Trans. Trans. Electrochem. Soc. **72**, 167 (1937).
 - [5] G.P. Thompson and M. Blackman, British Patent **817681** (1946).
 - [6] M. Glicksman and M. C. Steele, Phys. Rev. Lett. **2**, 461 (1959).
 - [7] M. Glicksman and R.A. Powlus, Phys. Rev. **121**, 1659 (1961).
 - [8] A.G. Chynoweth and A.A. Murray, Phys. Rev. **123**, 515 (1961).
 - [9] B. Ancker-Johnson and J.E. Drummond, Phys. Rev. **131**, 1961 (1963); **132**, 2372 (1963).
 - [10] M. Toda and M. Glicksman, Phys. Rev. **140**, A1317 (1965).
 - [11] K. Ando, J. Phys. Soc. Japan **21**, 1295 (1966).
 - [12] K. Hubner and L. Blossfeld, Phys. Rev. Lett. **19**, 1282 (1967).
 - [13] K. Ando and M. Glicksman, Phys. Rev. **154**, 316 (1967).
 - [14] K. S. Thomas, Phys. Rev. Lett. **23**, 746 (1969).
 - [15] W.S. Chen and B. Ancker-Johnson, Phys. Rev. B **2**, 4477 (1970).
 - [16] M. Glicksman, Jap. J. Appl. Phys. **3**, 354 (1964).
 - [17] H. Schmidt, Phys. Rev. **149**, 564 (1966).
 - [18] B.V. Paranjape, J. Phys. Soc. Jpn. **22**, 144 (1967).
 - [19] W.S. Chen and B. Ancker-Johnson, Phys. Rev. B **2**, 4468 (1970).
 - [20] K.v. Klitzing, G. Dorda, and M. Pepper, Phys. Rev. Lett. **45**, 494 (1980).
 - [21] D.C. Tsui, H.L. Stormer, and A.C. Gossard, Phys. Rev. Lett. **48**, 1559 (1982).
 - [22] For an extensive review of electronic, optical, and transport phenomena in the systems of reduced dimensions, such as quantum wells, quantum wires, quantum dots, and electrically/magnetically modulated 2DEG, see M.S. Kushwaha, Surf. Sci. Rep. **41**, 1 (2001).
 - [23] B. Tanatar, Solid State Commun. **92**, 699 (1994).
 - [24] J.S. Thakur and D. Neilson, Phys. Rev. B **56**, 4671 (1997).
 - [25] S. Das Sarma and E.H. Hwang, Phys. Rev. B **59**, 10730 (1999).
 - [26] L.J. Slater, *Confluent Hypergeometric functions* (Cambridge, London, 1960); M. Abramowitz and I.A. Stegun, *Handbook of Mathematical Functions* (Dover, New York, 1972); J. Spanier and K.B. Oldham, *An Atlas of Functions* (Springer-Verlag, Berlin, 1987).
 - [27] L.N. Pfeiffer, Private Communication.
 - [28] H. Alfvén, Arkiv för Matematik, Astronomi, och Fysik **39**, 2 (1943).
 - [29] M.S. Kushwaha, J. Appl. Phys. **109**, C106102 (2011).